J. Biochem. 132, 927–933 (2002)

Crystal Structure of Bovine Trypsin and Wheat Germ Trypsin Inhibitor (I-2b) Complex (2:1) at 2.3 Å Resolution[1]

S. Shanmuga Sundara Raj,[*,†] Eiji Kibushi,[†] Tatsuhiro Kurasawa,[†] Atsuo Suzuki,[†] Takashi Yamane,[†,2] Shoji Odani,[‡] Yugo Iwasaki,[§] Tsuneo Yamane,[§] and Tamaichi Ashida[†]

[*]Venture Business Laboratory, Nagoya University, Chikusa-ku, Nagoya 464-8603; [†]Department of Biotechnology, Graduate School of Engineering, Nagoya University, Chikusa-ku, Nagoya 464-8603; [‡]Department of Biology, Faculty of Science, Niigata University, Igarashi 2 no cho, Niigata 950-2181; and [§]Department of Biological Mechanisms and Functions, Graduate School of Bioagricultural Sciences, Nagoya University, Chikusa-ku, Nagoya 464-8601

Received July 10, 2002; accepted September 27, 2002

The Bowman-Birk trypsin inhibitor (BBI) from wheat germ (I-2b) consists of 123 amino acid residues with two inhibitory loops. The crystal structure of a bovine trypsin-wheat germ trypsin inhibitor (I-2b) complex (2:1) has been determined at 2.3 Å resolution to a final *R*-factor of 0.177. A distance of 37.2 Å between the contiguous contact loops allows them to bind and inhibit two trypsin molecules simultaneously and independently. Each domain shares the same overall fold with 8 kDa BBIs. The five disulfide bridges in each domain are a subset of seven disulfide bridges in the 8 kDa BBIs. I-2b consists of ten β-strands and the loops connecting these strands but it lacks α-helices. The conformations of the contiguous contact loops of I-2b are in a heart-like structure. The reactive sites in both domains, Arg 17 and Lys 76, are located on the loop connecting anti-parallel β-strands, β1/β2 and β6/β7. Strands β1 and β6 are in direct contact with trypsin molecules and form stable triple stranded β-sheet structures *via* hydrogen bonds.

Key words: Bowman-Birk type inhibitor, contiguous contact loop, double-headed inhibitor, trypsin inhibitor, wheat germ.

Plant seeds contain a large number of different types of serine protease inhibitors, which block trypsin and chymotrypsin of animal, fungal, and bacterial origins. Among many types of protease inhibitors from plants, Kunitz-type and Bowman-Birk type inhibitors (BBIs) have been studied most extensively. Members of the Kunitz-type inhibitor family have a molecular mass of about 20 kDa and two disulfide bridges, whereas those of the Bowman-Birk family are smaller (typically ~7 or ~14 kDa) and richer in disulfide bonds at evolutionarily conserved sites (*1*). BBIs that specifically inhibit trypsin or chymotrypsin have attracted much interest due to their anticarcinogenic activities (*2*) and immune-stimulating properties (*3*). Human populations consuming a large amounts of BBI in their diet have been shown to exhibit lower rates of colon, breast, prostate, and skin cancers (*4*). BBIs are double-headed inhibitors consisting of two domains formed by the tandem repeat of homologous amino acid sequences.

Some trypsin inhibitors have been isolated and characterized from tissues of gramineous plants, such as barley rootlet (*5*) and rice bran (*6*). Barley rootlet trypsin inhibitor (BRTI, M_r = 13,826) is a double-headed inhibitor composed of 124 amino acid residues with 10 disulfide bridges. It shows an intramolecular sequence identity of 55% between the N-terminal half (residues 1–62) and C-terminal half (63–124), and each half has a reactive site suggesting that this inhibitor may have originated from a duplicated form of a single-headed inhibitor with a M_r of about 8,000 (*5*). Rice bran trypsin inhibitor (RBTI) is also homologous to BRTI (*6*) and consists of 133 amino acid residues with 9 disulfide bridges.

Two groups of trypsin inhibitor from wheat germ, Group I (M_r=12,600, about 123 amino acid residues) and Group II (M_r=6,500, about 61 residues) were isolated and classified on the basis of molecular size by Odani *et al.* (*7*). Three-dimensional structures of several Group II BBIs have been reported, including the structures of peanut inhibitor A-II (*8*), soybean inhibitor (*9*), and pea seed inhibitor PsTI-IVb (*10*), which have been analyzed in the free form, as well as inhibitors from adzuki bean (*11*) and mung bean (*12*), which were determined in complex form with trypsin. However, only one crystal structure of a group I inhibitor, a 16 kDa BBI from barley seeds (BBBI) in the free form, has been reported at 1.9 Å resolution (*13*). Group I inhibitors are also highly homologous to the double-headed BBIs of leguminous plants. Group II inhibitors are single-headed trypsin inhibitors that contain only one of the two inhibitory domain structures of BBIs.

The two classes of inhibitors, groups I and II, show a high degree of sequence homology despite their different molecular sizes. The present paper describes the three-di-

[1] This work was supported in part by Grants-in-Aid for Scientific Research on Priority Areas (Nos. 05244102, 07554059) from the Ministry of Education, Science, Sports and Culture of Japan. X-ray data collection has been performed with the approval of the Photon Factory Advisory Committee (Proposal Nos. 92-045, 93G045).

[2] To whom correspondence should be addressed. Tel: +81-52-789-3339, Fax: +81-52-789-3218, E-mail: yamane@hix.nagoya-u.ac.jp

Abbreviations: BBI, Bowman-Birk type proteinase inhibitor; M_r, molecular weight; PDB, Protein Data Bank; BRTI, barley rootlet trypsin inhibitor; RBTI, rice bran trypsin inhibitor; BBBI, Bowman-Birk trypsin inhibitor from barley seeds.

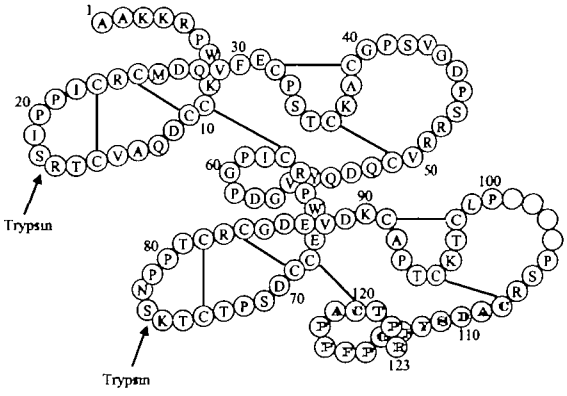

Fig. 1. **The amino-acid sequence of I-2b from wheat germ.** Black letters indicate the sequences analyzed chemically (*7, 23*) and outlined letters indicate sequences determined from the electron density map at 2.3 Å resolution.

mensional structure of I-2b, an important member of group I, in complex with bovine β-trypsin determined by molecular replacement methods at 2.3 Å resolution. The amino acid sequence of I-2b and the contiguous contact positions are shown in Fig. 1. This structure provides insight into the interaction between I-2b and trypsin inhibitor.

EXPERIMENTAL PROCEDURES

Crystallization, Data Collection and Processing—Wheat germs, kindly donated by Nippon Flour Mills, were defatted with cold (–20°C) acetone and ground finely. Bovine trypsin was obtained from Cooper Biomedical, USA. The purified I-2b was obtained through affinity chromatography and reverse phase high performance liquid chromatography. Crystallization was carried out by the hanging-drop vapour-diffusion method (*14*). Each droplet was composed of 5 μl of an aqueous solution containing 20 mg/ml protein and an equal amount of reservoir solution. Pillar-shaped crystals as large as 0.2 × 0.2 × 1.2 mm^3 were obtained within two weeks when 50 mM sodium phosphate buffer at pH 7–8 was used as the reservoir solution and 8–10% (w/v) polyethylene glycol 4000 with 1–3% (w/v) 1,4-dioxane was used as a precipitant. X-ray data were collected using a Sakabe's Weissenberg camera (*15*), at the BL6A2 station at the Photon Factory, National Laboratory for High Energy Physics. Two X-ray data sets, collected around the c^* and b^* axis, respectively, were processed using the *WEIS* program system (*16*). Table I presents a summary of data collection and processing. R_{merge} was 0.130 for 26,565 independent reflections of the merged data with $I > \sigma(I)$, where I_{hi} and I_h are the intensity and the mean, respectively, of the i-th observation of a reflection h. The completeness of the data set was 90.6% and that for the final resolution shell (2.38–2.30 Å) was 50.8%. The crystals belong to orthorhombic space group $P2_12_12_1$ with a = 73.49, b = 120.56, c = 70.04 Å and $V = 6.21 \times 10^5$ $Å^3$. One I-2b and two trypsin molecules are in an asymmetric unit, producing a V_m (*17*) of 2.58 $Å^3$/Da.

Molecular Replacement—The rotational (R) and translational (T) parameters of the two bovine trypsin molecules in the unit cell were determined using the fast-rotation function (*18*) and T1 function (*19*), respectively. Initially, the

TABLE I. **Data collection statistics.**

	Rotation axis	
	c^*	b^*
Wavelength (Å)	1.00	1.00
Oscillation angle (°)	7–2	5
Overlap angle (°)	0.5	0.5
Total rotation angle (°)	95	95
Exposure time (s/°)	10	4–8
Number of films	27	21
Resolution (Å)	2.4	2.3
Total reflections	66,175	77,492
Independent reflections with $I > \sigma(I)$	21,704	23,849
R_{merge} †	0.075	0.082

†$R_{merge}=(\Sigma_h\Sigma_i|I_h-I_{hi}|)/(\Sigma_h I_{hi})$, where I_{hi} and I_h are the intensity and mean, respectively, of the i-th observation of a reflection h. The value of R_{merge} for the merged data was 0.130 for 26,565 independent reflections.

rotational and translational parameters of only one trypsin molecule (Trypsin A) were obtained using the structure of bovine trypsin (PDB entry 2PTN) as a search model. Data from 6.0 to 3.5 Å resolution provided the best results. An unambiguous peak was located at ϕ = 86, ψ = 198, χ = 47°, and at x = 0.184, y = 0.042, z = 0.418 in each function. Using the amplitude,

$$||F_{obs}|-k|F_{cal,trypsin}||$$

where $F_{cal,trypsin}$ is the calculated structure factor of the first located trypsin molecule, and the scale factor k is estimated using

$$(\Sigma|F_{obs}|/\Sigma|F_{cal,trypsin}|) \times (M_r \text{ of trypsin}/M_r \text{ of complex}),$$

and by taking the first trypsin molecule into consideration, the fast-rotation function showed the orientation of the second trypsin molecule (Trypsin B) to have the highest peak at ϕ = 20, ψ = 33, and χ = 210°. The height of the highest noise peak was only 65% of the true peak. The positional parameters of Trypsin B could be obtained uniquely at x = 0.264, y = 0.600, and z = 0.339, by applying the translation function on this difference Patterson map.

Model Building and Refinement—The structures of the two trypsin molecules were first refined by the program *PROLSQ* (*20*) to an R-factor of 0.310 for 11,691 reflections [$F_{obs} > 3\sigma(F)$] in the resolution range of 7.0–3.0 Å. A total of 5% of the measured data were marked for a test set to calculate the free R-factor. After refitting the two trypsin molecules to the electron density using the *Turbo-FRODO* graphics program system (*21*), the R factor for the 7.0–2.5 Å resolution was decreased to 0.293. However, the electron density map synthesized using ($|F_{obs}|-|F_{cal}|$) coefficients at this stage was still inadequate to build a model of I-2b. Since only the N-terminal sequence was known at first, those residues were first identified and the C-terminal half was built as polyalanyl peptide chains. The identification of ten disulfide bridges was helpful in connecting the secondary structural elements. Simulated annealing using the standard slow cooling protocol was performed using the *X-PLOR* program (*22*). Refinement was interlaced with the model-building sessions using the program *Turbo-FRODO*. The final model could be determined from the electron density maps at 2.3 Å resolution. For the identification of solvent molecules, F_o–F_c difference maps were searched for the highest peaks. A total of 223 water molecules were

finally included.

In the final stage of the refinement, the electron density for the N-terminal 4 residues and the 4 residues from 101 to 104 in a surface loop region were too weak to build the models of these two peptide segments. There might be a possibility of breaking the chain from residues 101 to 104 when the native protein is exposed to trypsin because of the two Arg residues (102 and 104) in that highly mobile loop region.

In the early stages of structure solution only the 56 N-terminal amino acid residues of I-2b were known (*7*). The rest of the sequence was built from the election density maps. Later, the sequence analysis of 107 residues became available (Iwasaki, Y. and Yamane, T., unpublished results). The sequences known and those determined from the electron density matched quite well. The C terminal residues beyond 107 residues were determined very clearly from the electron density maps taking into consideration the amino acid composition of I-2b and the sequences of similar inhibitors.

RESULTS AND DISCUSSION

Quality of the Structure—The final complex model includes 4,120 protein atoms (862 atoms for the 115 residues of I-2b and 1629 atoms for each trypsin) and 223 water molecules. The final working and free *R*-factors were 0.177 and 0.241, respectively, for 24,253 reflections with a $3\sigma(F)$ cut-off between 9 and 2.3 Å resolution. The mean *B* factors for overall protein, main-chain and side-chain atoms were: 40.6, 39.3, and 42.0 Å^2 for I-2b; 22.0, 22.5, and 21.6 Å^2 for Trypsin A; 37.1, 37.6, and 36.1 Å^2 for Trypsin B; 32.4, 31.9, and 33.0 for the complex, respectively, while that of 223 water molecules was 45.7 Å^2. In the Ramachandran plot (*23*) of the complex 86.4% of the (ϕ, ψ) pairs lie in the allowed regions and all remaining pairs lie in the additionally allowed region. In the case of I2-b, out of 88 non-glycine residues, 76 (86.4%) are in the most favoured regions, 11 (12.5%) are in additionally allowed regions, and 1 (1.1%) residue in the generously allowed region, with no residues in the disallowed region (Fig. 2). From the Luzatti plot (*24*), the estimated coordinate error was found to be less than 0.28 Å. The stereochemistry of the model was verified using the software package *PROCHECK* (*25*), and no unreasonable geometry was observed.

Overall Structure of the Complex—In the crystal, I-2b binds with two molecules of trypsin, named "Trypsin A" and "Trypsin B," at Arg17 and Lys76, respectively. The C$^\alpha$ backbone of the complex and the ribbon diagram (*26*) with the reactive-site residues are shown in Fig. 3. The overall shape of the complex looks like an elongated cylinder with molecular dimensions of 90 × 45 × 36 Å. The structure of I-2b folds into two similar compact domains (domains N and C), each with approximately 60 residues. The molecule is almost symmetrical about the pseudo twofold axis passing through the center of the loop joining domains N and C. Two trypsin molecules are located at the end of the complex molecule without any interaction between them. Interestingly, the distance between the two reactive-site residues, 37.2 Å, is very similar to that of the 8 kDa BBIs in free form (36–40 Å). This enables I2-b to bind and inhibit two trypsin molecules simultaneously and independently. The relative orientation of the two domains of I-2b observed in this structure is much different from the dimeric arrangement in the crystal structure of PsTI-IVb (*10*). The two contiguous regions (*27*) (Arg17-Ser18 and Lys76-Ser77) are located at opposite sides of the inhibitor structure on protruding loops between strands β1 and β2 in the N domain (β6 and β7 in the C domain).

The structures of Trypsins A and B are essentially identical with a root mean square deviation (rmsd) of 0.32 Å for the equivalent C$^\alpha$ atoms. Interestingly, the mean *B* factor of Trypsin A, 22.0 Å^2, is significantly smaller than that of Trypsin B, 37.1 Å^2. This seems to be the primary reason why the orientation of Trypsin A was uniquely determined, whereas that of Trypsin B could not be determined simultaneously. The equivalent C$^\alpha$ atoms of Trypsins A and B have rmsd of 0.36 and 0.40 Å, respectively, compared to those of the initial trypsin model (PDB entry 2PTN).

Molecular Structure of I-2b—The I-2b structure with high proportions of cysteine and proline, only one methionine and no histidine residues consists of 10 β-strands and the loops connecting these β-strands with no α-helix (Fig. 4). It folds into two compact domains (termed N and C). The schematic diagram of I-2b shows that each domain, *i.e.*, domain N (residues 1–62) and domain C (residues 63–123), is separated into two subdomains; N1 (residues 13–25) and N2 (residues 39–51) for domain N, and C1 (residues 72–84) and C2 (residues 98–108) for domain C. The five disulfide bridges in each domain (9:63, 10:25, 15:23, 32:39, 36:51 in the N domain and 68:122, 69:84, 74:82, 91:98, 95:108 in the C domain) are a subset of the seven disulfide bridges in 8 kDa BBIs. Each domain consists of five β-strands. The triple stranded anti-parallel β-sheets formed by β1, β2, and β5 in subdomain N1 and β3 and β4 in subdomain N2 have similar conformations as the sheets formed by β6, β7, and β10 in subdomain C1 and β8 and β9 in subdomain C2, respectively. In addition to the hydrogen bonds between strands β1 and β2, two disulfide bridges between Cys10 and Cys25 and between Cys15 and Cys23 provide firmness in the sheet structure. Similarly, two disulfide bridges between Cys69 and Cys84 and between Cys74 and Cys82 firm the β6 β7 sheet. The reactive sites, Arg17 and Lys76,

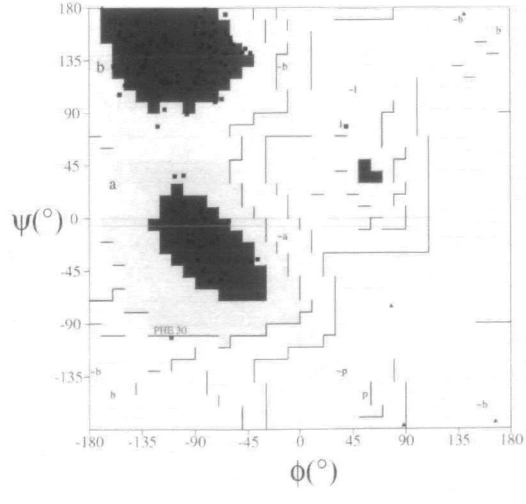

Fig. 2. **Ramachandran plot of I-2b.** The regions A, B, and L are most favoured, regions a, b, l, and p are allowed, and ~a, ~b, ~l, and ~p are the generously allowed regions. Glycine residues are represented as triangles.

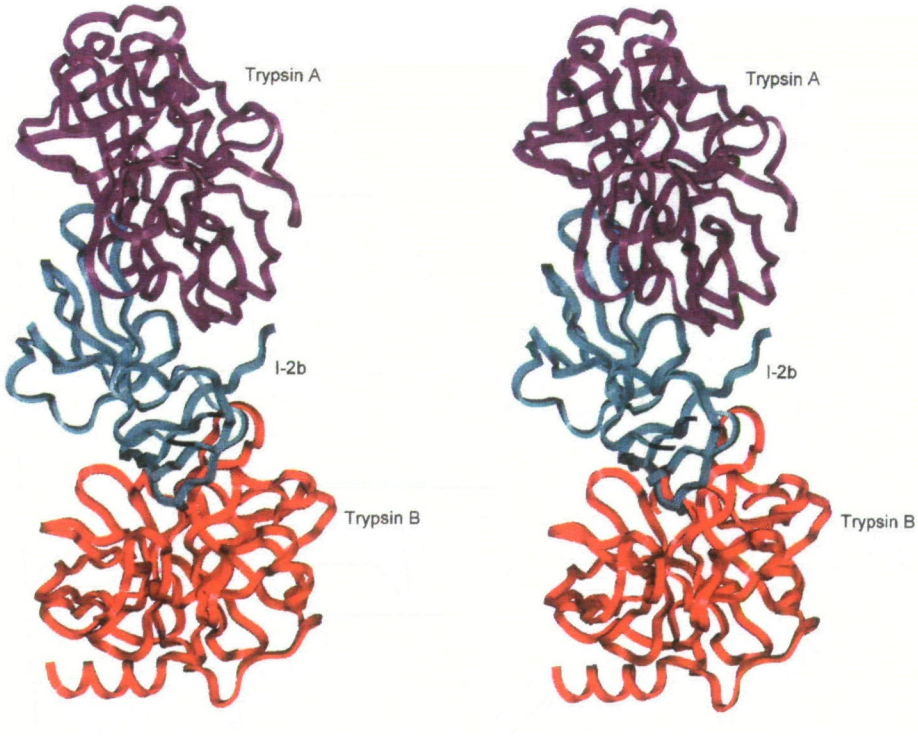

(a)

Fig. 3. **(a) Stereo view of the Cα backbone model of the 2:1 complex between trypsin and I-2b. (b) The ribbon diagram showing the reactive-site residues of I-2b and the interaction with the trypsin molecules.** Arrows represent the β-strands. Arg17 and Lys76 are shown. This figure was drawn by MOLSCRIPT (*26*).

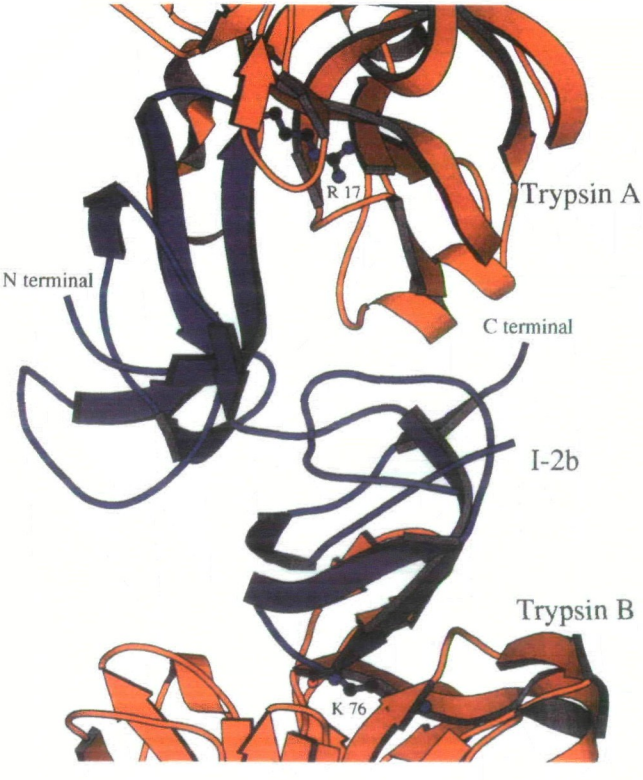

(b)

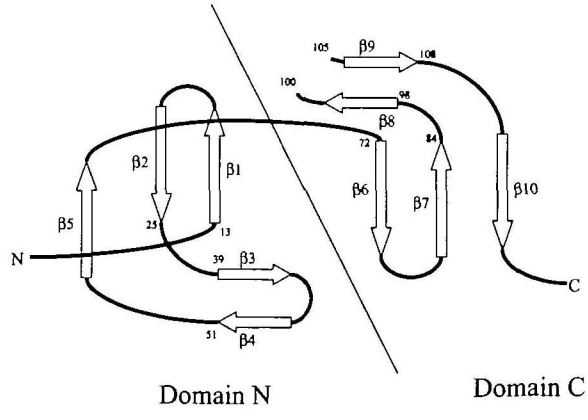

Fig. 4. **Schematic drawing of I-2b showing the domains, subdomains and β-strands.** Residues 101–104 could not be constructed because of the poor electron density map in that highly mobile region.

are located on the loops between β1 and β2 in domain N and between β6 and β7 in domain C, respectively. Domains N and C are covalently connected by a loop (residues 60–70) and a disulfide bridge between Cys9 and Cys63.

The superposition of the two domains (Fig. 5) gives an overall rmsd of 0.92 Å by a least-squares fitting of 38 common Cα atoms. I-2b shows an intramolecular sequence identity of 55% between the N and C domains. The reactive sites superpose well, showing the high degree of similarity between them. The largest differences were found in the surface loops between β3 and β4 and between β8 and β9, which also show relatively high B-factors, suggesting conformational flexibility in these loop regions. In the case of 8 kDa BBIs from leguminous seeds, an extra disulfide bond reduces the flexibility of the second reactive loop. The Cα atom of Pro100 in the loop between β8 and β9 is 3.49 Å away from that of Pro41 in the superimposed structure.

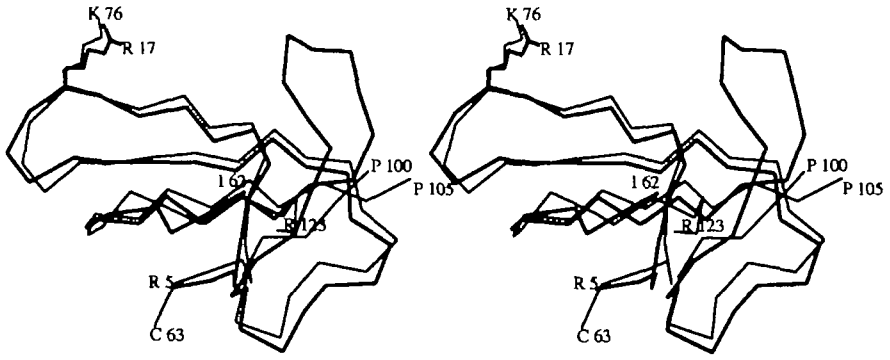

Fig. 5. **Stereoview of the superposition of domain N (thick lines) and domain C (thin lines).** They superpose well in the reactive-site region and deviations are observed in the loop regions.

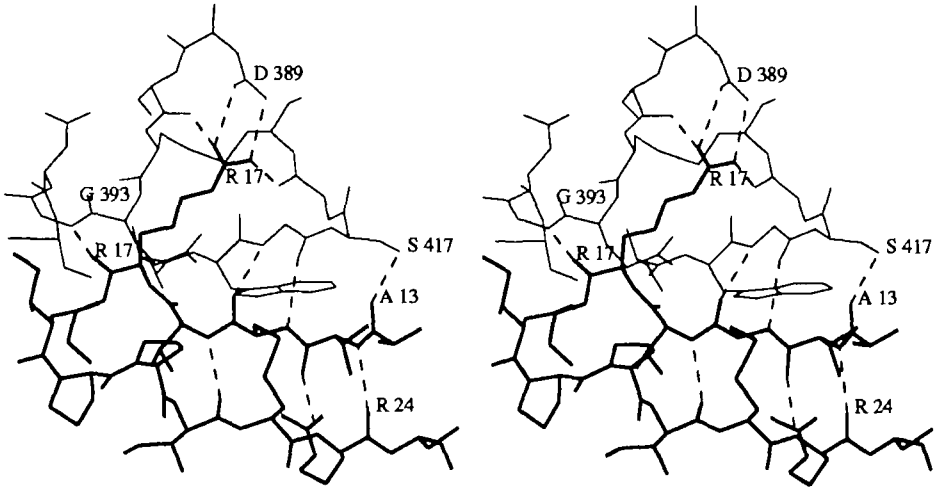

Fig. 6. **Stereoview of the intermolecular interactions between domain N of I-2b (thick lines) and trypsin A (thin lines).** The interactions form a triple stranded sheet structure.

The maximum deviation of 4.68 Å occurs between the C^{α} atoms of Pro105 and Arg48. These facts suggest that the fragment 101–104 is removed by proteolysis. The reactive loop between Cys15 and Cys23 has the same structure as the other reactive loop Cys74–Cys82.

Contiguous Contact Loops—Each of the two contiguous contact loops of I-2b is constrained by a disulfide bridge at its extremity (Cys15–Cys23 in the N-domain and Cys74–Cys82 in the C-domain). The hydrogen bonding network involving Thr16 and Ser18 in the N-domain and Thr75 and Ser77 in the C-domain causes the contiguous contact loop to adopt a heart-like shape (*11*). The contiguous contact loops of some protease inhibitors are relatively flexible in the free form, but become less mobile upon binding to protease. This is reflected by the reduction of the *B*-factors of the contiguous contact loop in the complex. This scheme is similar to those found in the other reactive site of I-2b and in the 1:1 complex between trypsin and adzuki inhibitor AB-I (*11*). Again, both the tight interaction within the reactive loop and the formation of the triple stranded β-sheet structure between BBI and trypsin appear to lower the *B* factors of the contiguous contact loops and prevent the necessary structural change of the inhibitor during proteolysis.

A triple stranded β-sheet formed by β1, β2, and a strand of Trypsin A (Ser414–Ser417) is clearly shown in Fig. 6. Strand β1 of I-2b, Val13–Thr16, is in direct contact with trypsin at strand Ser414–Ser417. The side chain of the reactive site, Arg17, appears clearly in the electron density map and is correctly positioned in the substrate specificity pocket of the trypsin molecule. This interaction pattern between domain C and Trypsin B is identical to that between domain N and Trypsin A.

Comparison with Other Inhibitor Structures—Sequence comparisons of I-2b with BBBI, BRTI, RBTI, and BBI are shown in Fig. 7. The amino acid sequence of I-2b as partially determined from the electron density map is compared to those of other trypsin inhibitors of the same family and found to show nearly 86% identity with BBBI and BRTI and 51% with RBTI. Comparison of the known amino acid sequence of the 56 N-terminal residues of I-2b, a group I inhibitor, with those of the 53 N-terminal residues of group II members, revealed a high degree of sequence identity. This duplication of domains may be regarded as the evolution of the inhibitor family.

The contiguous contact loops (residues Cys15–Cys23 and Cys74–Cys82) are the most conserved regions of BBI sequences. Disulfide bridges are also well conserved. It can be seen that structure variability is greater for regions that are not involved in protease recognition. Large deviations in these regions (residues Gly40–Arg49 and Leu99–Cys108 in the N and C domains, respectively) are due to the loss of disulfide bridges and to high B-factors. Therefore, they are more divergent in tertiary structure as well as in primary structure among BBIs. In the surface loop of subdomain N2, eleven residues are present between Cys39 and Cys51,

```
          1         10        *  20        30        40
I-2b  AAKKRPWKCCD--QAVCTRSIPPICRCMDQ-VF-ECPSTCKACGP
BBBI  AGKKRPWKCCD--EAVCTRSIPPICTCMDE-VF-ECPKTCKSCGP
BRTI  ADKKRPWKCCD--EAVCTRSIPPICTCMDE-VF-ECPKTCKSCGP
RBTI    MERPWKCCDNIKRLPTKPDPPQWRCNDELEPSQCTAACKSCRE
BBI    DDESSKPCCD--QCACTKSNPPQCRCSDM-RLNSCHSACKSC
                        |←  §  →|

                   50        60        70        80
I-2b  SVG-DPSRRVCQDQYVG-DPGPIC--RPWE-CCDSPTCTKSNPPT
BBBI  SMG-DPSRRICQDQYVG-DPGPIC--RPWE-CCDKAICTRSNPPT
BRTI  M-G-DPSRRICQDQYVG-DPGPIC--RPWE-CCDKAICTRSNPPT
RBTI  APGPFPGKLICEDIYWGADPGPFCTPRPWGDCCDKAFCNKMNPPT
BBI                                     ICALSYPAQ
                                        |←  §

                   90        100       110       123
I-2b  CRCGDEVDKCAPTCKTCLP (4residues) PSRCADSYFGPFPPAGTPR
BBBI  CRCVDEVKKCAPTCKTCLPSRSR-PSRRVCIDSYFGPVPPRCTPR
BRTI  CRCVKEVKKCAPTCKTCLPSRSR-PSRRVCIDSYFGPVPPRCTPR
RBTI  CRCMDEVKECADACKDCQRVESSEP-RYVCKDRFTGHPGPVCKPR
BBI   CFCVDITDFCYEPCKPSEDDKEN
      →|
```

Fig. 7. **Comparison of the amino acid sequences of I-2b, Bowman-Birk trypsin inhibitor from barley seeds (BBBI), barley rootlet trypsin inhibitor (BRTI), rice bran trypsin inhibitor (RBTI), and soybean Bowman-Birk type proteinase inhibitor (BBI).** Residues that coincide to those of I-2b at each position are shaded. Underlined positions indicate unknown sequences of I-2b. Symbols * and § denote reactive sites and reactive loops, respectively. Soybean BBI is a trypsin-chymotrypsin inhibitor.

whereas only nine residues are present between Cys98 and Cys108 in domain C. In the case of BBBI, BRTI, and RBTI, there are eleven residues in the corresponding loop region, Cys98–Cys108, of I-2b.

Structural Comparison of I-2b with BBBI—I-2b and BBBI, the only 16 kDa inhibitor solved in free form by X-ray crystallography, have a structural identity of more than 86%. Both structures consist of only β-sheets with no α-helix. The dimensions of I-2b are 52 × 50 × 25 Å. The superposition of the two molecules and the N and C domains are shown in Fig. 8. In both structures, the contiguous contact loops and disulfide bonds are conserved. The contiguous contact loop of a protease inhibitor is relatively flexible in its free state and becomes less mobile upon binding to target proteases. However, it should be noted that this is not accompanied by any significant structural change in the contiguous contact loop. The overall B-factor of the contiguous contact loops of BBBI is relatively low even in the free state. This may be partly due to the stabilization of the contiguous contact loops through intermolecular contacts with the symmetry-related molecules in the crystal.

Structural studies of I-2b and BBBI confirm and extend the early observations that all inhibitors have a largely exposed combining loop surrounding the P1 and P2 residues (*27*). The torsion angles of the combining loops are common to the inhibitors and remain the same in the complexes as well. [ϕ(P1) = –107 (–87); ψ(P1) = 36 (79); ϕ(P1′) = –86 (–144); ψ(P1′) = 172 (164) and ϕ(P2) = –99 (–87); ψ(P2) = 36 (–5); ψ(P2′) = –89 (–70); ψ(P2′) = 165 (160), P1=Arg17 (Arg17); P2 = Lys76 (Arg76), P1′ and P2′ = Ser18 and Ser77 for I-2b and BBBI; the values in parentheses are for BBBI and the others are for I-2b]

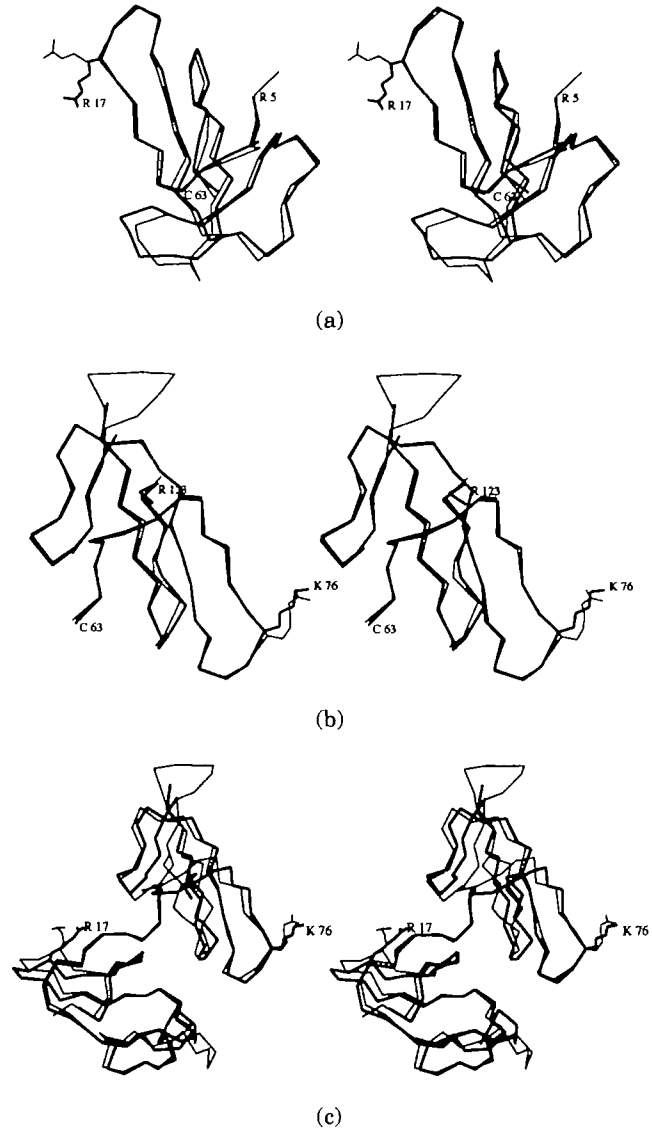

Fig. 8. **The superposition of (a) N and (b) C domains and (c) I-2b (thick) and BBBI (thin) molecules. Stereoviews.**

The modelling simulation of BBBI indicates that each of the two exposed contiguous contact loops readily slots into the active-site cleft of bovine pancreatic trypsin. In that model of the 1:2 complex, the bound trypsin molecules come very close, making van der Waals contacts with each other. This is in contrast with the I-2b complex where there is no interaction between the two trypsin molecules. The trypsin molecules are approximately 35 Å apart, thereby allowing the contiguous contact loops to bind and inhibit independently.

SSSR thanks Venture Business Laboratory, Nagoya University for the award of a Post-Doctoral Fellowship. We are grateful to Mr. Isoji Suzuki, Nippon Flour Mills, for providing wheat germ. We thank Dr. Tsuyoshi Shirai for critical reading of the manuscript.

REFERENCES

1. Birk, Y. (1987) Proteinase inhibitors in *Hydrolytic Enzymes* (Neuroberger, A. and Brocklehurst, K., eds.) pp. 257–300, Elsevier Science Publishers B.V., Amsterdam
2. Kennedy, A.R. (1993) Anticarcinogenic activity of protease inhibitors in *Protease Inhibitors as Cancer Chemopreventive Agents* (Troll, W. and Kennedy, A.R., eds.) pp. 9–64, Plenum Press, New York
3. Harms-Ringdahl, M., Forsberg, J., Fedorcsak, I., and Ehrenberg, L. (1979) Trypsin inhibitory activity of a polypeptide isolated from red kidney beans that also enhances lymphocyte stimulation. *Biochem. Biophys. Res. Commun.* **86**, 492–499
4. Birk, Y. (1993) Protease inhibitors of plant origin and role of protease inhibitors in human nutrition in *Protease Inhibitors as Cancer Chemopreventive Agents* (Troll, W. and Kennedy, A.R., eds.) pp. 97–106, Plenum Press, New York
5. Nagase, A., Fukamachi, H., Ikenaga, H., and Funatsu, G. (1988) The amino acid sequence of barley rootlet trypsin inhibitor. *Agric. Biol. Chem.* **52**, 1505–1514
6. Tashiro, M., Hasino, K., Shiozaki, M., Ibuki, F., and Maki, Z. (1987) The complete amino acid sequence of rice bran trypsin inhibitor. *J. Biochem.* **102**, 297–306
7. Odani, S., Koide, T., and Ono, T. (1986) Wheat germ trypsin inhibitors. Isolation and structural characterization of single-headed and double-headed inhibitors of the Bowman-Birk type. *J. Biochem.* **100**, 975–983
8. Suzuki, A., Yamane, T., Ashida, T., Norioka, S., Hara, S., and Ikenaka, T. (1993) Crystallographic refinement of Bowman-Birk type protease inhibitor A-II from peanut (*Arachis hypogaea*) at 2.3 Å resolution. *J. Mol. Biol.*, **234**, 722–734
9. Voss, R.-H., Ermler, U., Essen, L.-O., Wenzl, G., Kim, Y.-M., and Flecker, P. (1996) Crystal structure of the bifunctional soybean Bowman-Birk inhibitor at 0.28-nm resolution. *Eur. J. Biochem.* **242**, 122–131
10. de la Sierra, I.L., Quillien, L., Flecker, P., Gueguen, J., and Brunie, S. (1999) Dimeric crystal structure of a Bowman-Birk protease inhibitor from pea seeds. *J. Mol. Biol.* **285**, 1195–1207
11. Tsunogae, Y., Tanaka, I., Yamane, T., Kikkawa, J., Ashida, T., Ishikawa, C., Watanabe, K., Nakamura, S., and Takahashi, K. (1986) Structure of the trypsin-binding domain of Bowman-Birk type protease inhibitor and its interaction with trypsin. *J. Biochem.* **100**, 1637–1646
12. Li, Y., Huang, Q., Zhang, S., Liu, S., Chi, C., and Tang, Y. (1994) Studies on an artificial trypsin inhibitor peptide derived from the mung bean trypsin inhibitor: chemical synthesis, refolding, and crystallographic analysis of its complex with trypsin. *J. Biochem.* **116**, 18–25
13. Song, H.K., Kim,Y.S., Yang, J.K., Moon, J., Lee, J.Y., and Suh, S.W. (1998) Crystal structure of a 16 kDa double-headed Bowman-Birk trypsin inhibitor from barley seeds at 1.9 Å resolution. *J. Mol. Biol.* **293**, 1133–1144
14. Suzuki, A., Kurasawa, T., Tashiro, C., Hasegawa, K., Yamane, T., Ashida, T., and Odani, S. (1993) Crystallization and preliminary X-ray studies on the trypsin inhibitor I-2 from wheat germ and its complex with trypsin. *Acta Crystallogr.* **D49**, 594–596
15. Sakabe, N. (1983) A focusing Weissenberg camera with multilayer-line screens for macromolecular crystallography. *J. Appl. Cryst.* **16**, 542–547
16. Higashi, T. (1989) The processing of diffraction data taken on a screenless Weissenberg camera for macromolecular crystallography. *J. Appl. Cryst.* **22**, 9–18
17. Matthews, B.M. (1968) Solvent content of protein crystals. *J. Mol. Biol.* **33**, 491–497
18. Crowther, R.A. (1972) The fast rotation function in *The Molecular Replacement Method* (Rossmann, M.G., ed.) pp. 173–178, Gordon and Breach, New York
19. Lattman, E. (1985) Use of the rotation and translation functions in *Methods in Enzymology* (Wyckoff, H.W., Hirs, C.H.W., and Timasheff, S.N., eds.) Vol. 115, pp. 55–77, Academic Press, Orlando
20. Hendrickson, W.A. and Konnert, J.H. (1980) Incorporation of stereochemical information into crystallographic refinement in *Computing in Crystallography* (Diamond, R., Ramaseshan, S., and Venkatesan, K., eds.) pp. 13.01–13.23, Indian Academy of Sciences, Bangalore
21. Cambillau, C. (1992) *Turbo-FRODO*, Molecular Graphics Program for Silicon Graphics IRIS 4D Series, Version 3.0, Bio-Graphics, Marseille, France
22. Bruenger, A.T. (1990) *X-PLOR* Manual, Version 2.1, Yale Univ., New Haven, USA
23. Ramakrishnan, C. and Ramachandran, G.N. (1965) Stereochemical criteria for polypeptide and protein chain conformations. II. Allowed conformations for a pair of peptide units. *Biophys. J.* **5**, 909–933
24. Luzatti, P.V. (1952) Traitement statistique des erreurs dans la determination des structures cristallines. *Acta Crystallogr.* **5**, 802–810
25. Laskowski, R.A., MacArthur, M.W., Moss, D.S., and Thornton, J.M. (1993) *PROCHECK*: a program to check the stereochemical quality of protein structures. *J. Appl. Cryst.* **26**, 283–291
26. Kraulis, P.J. (1991) *MOLSCRIPT*: a program to produce both detailed and schematic plots of protein structures. *J. Appl. Cryst.* **24**, 946–950
27. Laskowski, Jr. M. and Qasim, M.A. (2000) What can the structures of enzyme-inhibitor complexes tell us about the structures of the enzyme substrate complexes? *Biochim. Biophys. Acta* **1477**, 324–337